# System dynamics revealed by recurrence quantification analysis: Application to molecular dynamics simulations

T. E. Karakasidis,* A. Fragkou, and A. Liakopoulos
*Department of Civil Engineering, University of Thessaly, Pedion Areos, 38334 Volos, Greece*
(Received 14 March 2007; published 24 August 2007)

The present work examines the applicability and efficacy of recurrence plots and recurrence quantification analysis in interpreting statistical-mechanics-based simulations of classical fluids and solids. We analyze temperature time series obtained from molecular dynamics simulations of a Lennard-Jones system at various fluid and solid states. It turns out that the structure of the recurrence plots reflects the different regimes of atomic motion as well as the degree of atomic diffusivity as the system density and temperature are varied. Recurrence plots (RPs) can help to localize a region where a phase transition occurs, while recurrence quantitative analysis descriptors confirm in a more clear way the results of RPs. The trends identified in our results are in qualitative agreement with direct computation of Lyapunov exponents for liquid Lennard-Jones systems reported in the literature.

DOI: 10.1103/PhysRevE.76.021120 PACS number(s): 05.20.Jj, 05.45.Tp, 02.70.Ns

## I. INTRODUCTION

The study of dynamical systems by analyzing the evolution in time of one or more observables is of importance in many scientific areas, since we rarely have direct access to the intrinsic dynamics of a system. Usually, we record one or more system observables at equidistant points in time and, based on the time series generated, we extract characteristics about the underlying system dynamics. This is the case in many physical systems in materials science, meteorology, hydrology, etc., as well as biology, econometrics, and financial analysis, to mention just a few scientific areas where time series analysis has attracted great interest in recent years, especially in cases where the behavior of the underlying system is chaotic.

Standard methods in time series studies include spectral analysis, rescaled range analysis, computation of autocorrelation functions, and average mutual information. More complex methods based on phase space reconstruction, such as computation of correlation dimension and the false nearest neighbors test are also very useful in time series analysis. Comprehensive reviews of these methods can be found in [1–3]. These methods allow us to extract information about system temporal correlations and to give an answer to the question of the existence or not of a chaotic attractor. However, these methods are not always straightforward to apply and must be used with caution, especially in applications with high noise-to-signal ratio, short observation records, and high dimensionality. More recent methods, based also on the idea of phase space, include the construction of recurrence plots (RPs) [4] (a visual analysis tool that relies heavily on the power of human perception) and the recurrence quantification analysis (RQA) [5] which extracts quantitative information from RPs in order to render the analysis objective.

In this paper, we focus on a dynamical system which consists of argon atoms interacting via a Lennard-Jones potential. The system evolution in time is simulated by classical molecular dynamics (MD) methods [6,7] at various thermodynamic states. Based on statistical mechanics one can compute a number of system "observables" such as temperature, pressure, potential energy, etc., i.e., measurable quantities that depend on the system dynamics. These highly oscillatory time series were analyzed by Karakasidis and Liakopoulos [8] using standard time series methods of analysis. Specifically, rescaled range analysis and spectral analysis revealed a two-regime power law ($1/f^{\alpha}$) behavior which corresponds to the regimes of atomic motion in the fluid. Posch and Hoover studied the full Lyapunov spectrum of such a Lennard-Jones fluid at various thermodynamic states and found it to be chaotic [9,10]. Giuliani and Manetti [11] and Manetti *et al.* [12] have employed RQA to discriminate the dynamics of proteins from the dynamics of a simple Lennard-Jones liquid by analyzing the potential energy time series generated by molecular dynamics simulations. That study was limited to only one state of the Lennard-Jones fluid.

In the present work, we use RPs and RQA to analyze a model Lennard-Jones system at various thermodynamics states in order to see how the inherent dynamics of the system is reflected in the RPs and the RQA descriptors. Molecular dynamics simulations were carried out in the microcanonical ensemble, and a single observable, the instantaneous temperature, was analyzed. We note that the instantaneous system temperature, being proportional to the kinetic energy, depends on the squares of the particle velocities and thus directly on the dynamics of the system. We mention also that an analysis of the instantaneous potential energy would not add new information because in the microcanonical ensemble the kinetic energy fluctuations are the same as those of the potential energy, since the sum of potential and kinetic energy is constant. This is expected on theoretical grounds [13], and it is also confirmed in our simulations for the system under study [8]. The temperature time series is used to reconstruct the phase space, and subsequent analysis of the results obtained shows how the dynamics of the physical system and its liquid-to-solid phase transition is reflected in the RP and RQA measures.

*thkarak@uth.gr

 

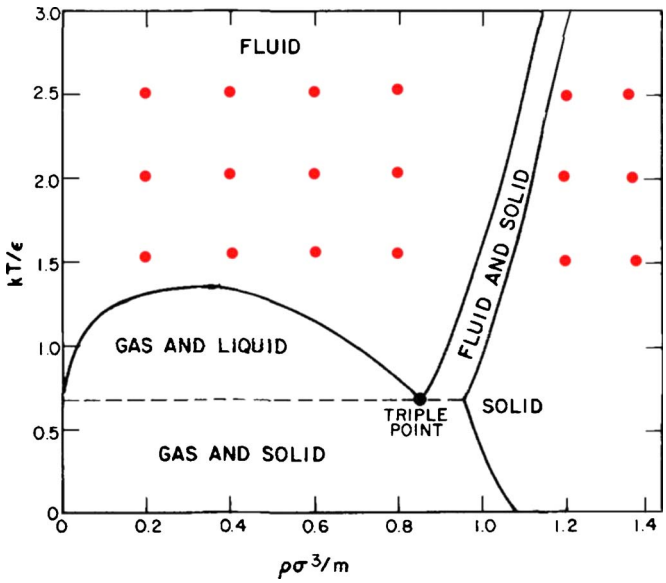


FIG. 1. (Color online) Phase diagram of the Lennard-Jones system (from [14]). The simulated states are marked in red.

The paper is organized as follows. In Sec. II a brief description of the molecular dynamics method along with a short presentation of the ideas behind the recurrence plots and recurrence quantification analysis are given. In Sec. III we present the analysis of temperature time series using RPs and RQA and attempt a physical explanation of the observed behavior. Conclusions are summarized in Sec. IV.

## II. MODELS AND METHODS

### A. Molecular dynamics simulations

We consider a system of $N_p$ interacting particles contained in a volume $V$. In the absence of external forces, the dynamics of the system is described by a Hamiltonian $H$ which is conserved in time, i.e.,

$$H = \sum_{i=1}^{N_p} \frac{1}{2} m_i v_i^2 + U(\vec{r}_1, \ldots, \vec{r}_{N_p}) = \text{const}, \tag{1}$$

where $\vec{r}_i$ and $\vec{v}_i$ denote the position vector and velocity of the $i$th atom, respectively. The sum in Eq. (1) represents the kinetic energy of the system while $U$ denotes the potential energy of the system.

In the present work, atomic interactions are described by a 6-12 Lennard-Jones potential:

$$\varphi(r_{ij}) = 4\varepsilon[(\sigma/r_{ij})^{12} - (\sigma/r_{ij})^6] \tag{2}$$

and $\sigma$ and $\varepsilon$ are parameters empirically derived by fitting calculated quantities to experimental data. For argon, the values of the parameters are $\sigma=3.408$ Å and $\varepsilon/k_B=119.8$ K. The cutoff distance for the interactions was set to $2.5\sigma$. It is customary to refer to the system reduced temperature, defined as $T^*=k_BT/\varepsilon$, and to reduced density, defined as $\rho^*=N_p\sigma^3/V$, where $N_p$ is the number of atoms in the MD cell and $V$ is the cell volume. The phase diagram of the Lennard-Jones system appears in Fig. 1 and the simulated thermodynamic states are marked.

For a system in three dimensions, we integrate $3N_p$ coupled second-order scalar differential equations of motion with appropriate initial conditions and determine the position and velocity of each particle as functions of time. Average temporal quantities, which are comparable to macroscopic measurable quantities, are computed through statistical mechanics relations [7], e.g., the instantaneous kinetic temperature is given by

$$T = \frac{1}{3N_p k_B} \sum_{i=1}^{N_p} m_i v_i^2, \tag{3}$$

where $v_i$ denotes the speed of particle $i$ and $k_B$ is the Boltzmann constant. Further in the text we are going to refer to this quantity as the system instantaneous temperature. In addition to the temperature time series, we have calculated and analyzed the mean square displacements (MSDs) which are defined as

$$\langle \delta r^2(t) \rangle = \frac{1}{N} \left\langle \sum_{i=1}^{N} [r(0) - r(t)]^2 \right\rangle \tag{4}$$

The symbol $\langle \cdots \rangle$ denotes an average in time. The MSD shows how far the atoms are displaced from their initial positions as a function of time.

Simulations were performed for $N_p=256$ atoms. In order to start the simulation, atoms are located on a fcc lattice in a cube with edges parallel to the directions $x$ [100], $y$ [010], and $z$ [001]. The dimensions of the simulation cell are such that we match the reduced density of the system. Periodic boundary conditions are applied in the $x$, $y$, and $z$ directions. The equations of motion were solved using Verlet's algorithm [15], with a time step $\delta t=10^{-14}$ s. In order to start the simulation, atoms are given velocities in order to reach the appropriate temperature conditions. Equilibration runs of $3 \times 10^4$ steps were performed before starting the production runs. The production runs were $10^{-10}$ s long and all relevant quantities were saved every $10^{-14}$ s. We simulated the system for reduced density $\rho^*$ in the range 0.2–1.4 and reduced temperature $T^*$ in the range 1.5–2.5 (see Fig. 1). At each thermodynamic state, results are averaged over ten independent production runs performed with different initial conditions.

### B. Recurrence plots and recurrence quantification analysis

Recurrence plots are a graphical tool introduced by Eckmann *et al.* [4] in order to extract qualitative characteristics of a time series. In the present work, the method is implemented in the reconstructed phase space of the system, but it can be applied to any phase space trajectory. We first embed the time series, say $x(t)$, in an $m$-dimensional space by forming a sequence of vectors $\mathbf{s}_i=\{x[t_i-(m-1)\tau_d], x[t_i-(m-2)\tau_d], \ldots, x(t_i)\}$, where $\tau_d$ denotes an appropriately selected time delay. The corresponding RP is based on the recurrence matrix [16]

$$R_{i,j} = \begin{cases} 1, & s_i \approx s_j, \\ 0, & s_i \neq s_j, \end{cases} \qquad i,j = 1, \ldots, N, \tag{5}$$

where $N$ is the number of considered states and $s_i \approx s_j$ signifies equality up to a cutoff distance $\varepsilon$. In fact, one compares the states of the system at times $i$ and $j$ and, if they are similar, this is indicated by a 1 in the recurrence matrix, otherwise the corresponding value is set to zero. The RP is obtained by plotting the recurrence matrix using different colors for its binary entries, e.g., plotting a black dot at coordinates $(i,j)$ if the corresponding element of the recurrence matrix is $R_{i,j}=1$ and a white dot for $R_{i,j}=0$. By definition $R_{i,i}=1$ for every $i$ and thus the RP has a black main diagonal line called the line of identity. Moreover, RPs are symmetric by definition with respect to the diagonal ($R_{i,j}=R_{j,i}$). When computing a RP, a norm must be chosen. The most frequently employed norms are the $L_1$ norm, the $L_2$ norm (Euclidean norm), and the $L_\infty$ norm (maximum or supremum norm) [16]. In the present study, we employed the Euclidean norm since it gives an intermediate number of neighbors compared to the $L_1$ and $L_\infty$ norms [16].

In the literature there are several variations of RPs. One of them, which is widely employed, consists of plotting the distance matrix

$$D_{i,j} = \|s_i - s_j\| \tag{6}$$

instead of plotting the recurrence matrix. Although this is not a RP *per se*, it is sometimes called a global recurrence plot [17] or an unthresholded recurrence plot [18]. The name "distance plot" would perhaps be most appropriate in this case, as mentioned in [16]. In this case, the pixels of the plot can be colored according to how large or small the distance $D_{i,j}$ is relative to the cutoff distance within which two state points are considered as recurrence points. In the present study, we employed such a color coding.

RPs exhibit large- and small-scale structure and different conclusions can be reached from examination at different scales. Hereafter we mention the basic indications and their relation to the underlying system behavior. For further details the reader may consult [4,16,19].

The large-scale structure can give the following indications.

(a) Homogeneous RPs represent stationary and autonomous systems for which relaxation times are short in comparison with the time spanned by the RP. Such RPs may occur for random time series.

(b) Periodic systems result in RPs with diagonally oriented, periodic recurrent structures such as diagonal lines or checkerboard structures.

(c) Systems with slowly varying parameters result in a RP characterized by a drift.

(d) Abrupt changes in the dynamics as well as extreme events result in white areas or bands in the RP.

The texture (small-scale structure), which may consist of single dots, or diagonal, vertical, or horizontal lines, is also indicative of distinct system behavior.

(a) Single, isolated recurrence points can occur if states are rare, if they do not persist for any time, or if they present important fluctuations. However, they are not a unique sign of chance or noise.

(b) A diagonal line occurs when a segment of the trajectory runs parallel to another segment, i.e., the trajectory visits the same region of the phase space at different times.

(c) A vertical or horizontal line marks a time length in which a state does not change or changes very slowly.

Although powerful as a visual interpretation aid, the RP is just a qualitative tool in order to obtain insight about the dynamical system. Webber and Zbilut [5] and Marwan *et al.* [20] extended this idea and defined a number of measurable quantities that can be extracted from the recurrence plots, giving rise to recurrence quantification analysis. RQA has been used in the study of various dynamical systems such as proteins [21,22], corrosion [23], financial systems [24,25], physiological systems [20,26,27], and traffic dynamics [28] just to mention a few. One advantage of RQA over other tools of analysis of time series is that it does not require that the time series under study is stationary.

Some of the RQA indices that have been proposed [5,20] and we have employed in the present study are summarized in the following paragraphs for easy reference.

*(a) Recurrence* ($\mathcal{R}_{\mathrm{Rec}}$, frequently referred to also as %REC) gives the ratio of the number of recurrence points (pixels) to the total number of points (pixels) of the plot,

$$\mathcal{R}_{\mathrm{Rec}} = \frac{1}{N^2} \sum_{i,j=1}^{N} R_{ij}. \tag{7}$$

This is a basic output of RQA. Its value depends on the cutoff radius chosen.

*(b) Determinism* ($\mathcal{R}_{\mathrm{Det}}$, or %DET) is the ratio of the number of recurrence points forming upward diagonal lines to the total number of recurrence points,

$$\mathcal{R}_{\mathrm{Det}} = \frac{\sum_{l=l_{\min}}^{N} lP(l)}{\sum_{l=l_{\min}}^{N} P(l)}. \tag{8}$$

The threshold $l_{\min}$ excludes the diagonal lines formed by the tangential motion of the phase space trajectory [16].

Periodic signals have very long uninterrupted diagonal lines; uncorrelated stochastic signals result in RPs with many single points, while chaotic signals have a broad distribution of lengths of diagonal lines [16].

*(c) Maxline*, which is simply the length of the longest diagonal line segment in the plot, excluding the main diagonal line of identity. This is a very important recurrence variable because it is related to the Lyapunov exponents [4,29]. As discussed extensively in [16], Eckmann *et al.* have stated that "the length of the diagonal lines is related to the largest positive Lyapunov exponent if any" [4]. One approach to estimate the largest Lyapunov exponent is to compute the largest line. However, the relationship between this measure and the positive Lyapunov exponent is more subtle, as discussed extensively in [16]. In fact, the $K_2$ entropy is related to the cumulative frequency distribution of the lengths of the

diagonal lines and therefore with the lower limit of the sum of positive Lyapunov exponents $K_2 \leqslant \Sigma_{\lambda,>0}\lambda_\iota$. Thus maxline can be used as an estimator of $K_2$ and thus of the lower limit of the sum of the positive Lyapunov exponents. As a consequence, the shorter the maxline, the "more chaotic" the time series.

*(d) Trapping time* ($\mathcal{T}_{\text{Time}}$, or TT) shows the average length of the vertical lines,

$$\mathcal{T}_{\text{Time}} = \frac{\sum_{v=v_{\min}}^{N} vP(v)}{\sum_{v=v_{\min}}^{N} P(v)} \tag{9}$$

where $v$ is the length of the vertical lines, $v_{\min}$ is the lowest length that is considered a line segment (which is usually taken to be equal to 2), and $P(v)$ is the distribution of the corresponding lengths. The TT shows the time that the system has been trapped in the same state. We stress the point that these measures are based on binary RPs.

### C. RPs and RQA: Implementation details

In order to construct the RPs and perform the RQA analysis, we employed the visual recurrence analysis (VRA) program of Kononov [30]. In order to construct a recurrence plot one has to reconstruct the phase space and thus one has to specify the embedding dimension and time delay. The time delay $\tau_d$ was determined by the first minimum of the average mutual information, which is a criterion widely employed in time series analysis [2]. The values of $\tau_d$ for the fluid states were in the range 10–17 simulation time steps, and for the solid in the range 4–6 time steps. We have chosen the embedding dimension to be 5 based on results from principal component analysis.

Another parameter that must be specified is the norm used to calculate the distances between the reconstructed phase space states (points). We have used the Euclidean norm throughout this work since it is widely employed in the literature and it gives an intermediate number of neighbors compared to the $L_1$ and $L_\infty$-norms [16].

The cutoff distance was chosen using Webber and Zbilut's [5] rule of thumb that $\mathcal{R}_{\text{Rec}}$ should be kept low (of the order of 0.1–2.0 %) which is also suggested by Marwan [19]. We have chosen cutoff values such that the resulting $\mathcal{R}_{\text{Rec}}$ was around 1%. This results in radii in the range 42–50 pixels. The lowest number of recurrence points required to define a deterministic line was taken to be 2 [5,19].

## III. RESULTS AND DISCUSSION

Representative RPs obtained at various system densities and temperatures are shown in Fig. 2. We first discuss qualitatively the recurrence characteristics of our system based on the RPs before presenting quantitative results using RQA. All RPs presented here are thresholded and the points that are considered recurrent are classified into categories (depending on the magnitude of the distance $D_{ij}$) and color coded as follows: Black and blue pixels represent system states (microstates) that are closest to each other in the reconstructed phase space, red pixels correspond to intermediate distances, while yellow pixels represent still "recurrent states" (i.e., points in the interior of the hypersphere $|D_{ij}| = \varepsilon$) but separated by even larger distances. On the other hand, gray points are nonrecurrence points, i.e., points in the exterior of hypersphere $|D_{ij}| = \varepsilon$.

A first qualitative conclusion that arises from the results summarized in Fig. 2 is that the lower the system density and temperature the more "structured" the RP appears to be. As the system density and temperature are raised, the structure is gradually lost and the RPs become more homogeneous at least at the scale of the plots in Fig. 2. For a given temperature, as the system density increases the number of dark-blue points decreases [Figs. 2(b), 2(d), 2(f), and 2(h)], while the number of red points increases.

At low density [Fig. 2(a)] there are relatively large regions of gray points (nonrecurrent states), and as density increases these gray regions get smaller and are distributed over the whole plot [Fig. 2(c) and 2(e)]. In the solid, gray points are distributed almost homogeneously over the plot [see Fig. 2(h)] resembling RPs of a random signal. High-density fluid states [Fig. 2(e)] give rise to RPs resembling more a solid state RP [Fig. 2(h)] than the RP of low-density fluid [e.g., Fig. 2(a)]. This characteristic change of the structure of the RP may be used to identify the phase of our system or discriminate a solid state from a liquid state.

On the other hand, for a given density, as the temperature increases we observe a similar change in the distribution of recurrence points. This behavior can be seen by comparing Figs. 2(a), 2(c), 2(e), and 2(h) with Figs. 2(b), 2(d), 2(f), and 2(g), respectively. We observe that the increase of temperature leads to loss of structure of the RP and to an increase of states that are classified as recurrent but with relatively large distances between them (red-colored points).

An understanding of the described evolution of the structure of the RPs can be obtained on physical grounds by considering the motion of the atoms in a liquid and in a solid. In a solid, atoms perform vibrations around their mean positions, while in the fluid phase, atoms perform a combination of diffusional and vibrational motion, the latter becoming predominant as the fluid density increases. The motion of atoms determines the microstates of the system in phase space.

If we concentrate on the motion of just one atom for simplicity, we can reason as follows. In the solid, the states of an atom are more or less related, since vibration around its ground state position does not result in any significant change in the energy and the atomic configuration. There is, of course, a loss of correlation when the atom changes direction of motion, and this occurs very often, practically at a half period of the vibration. Given that the characteristic time of vibrations is of the order of picoseconds, this results in temporal correlations of microstates of the order of $10^{-13}$ s or a few simulation time steps ($\delta t = 10^{-14}$ s). This is in fact the situation that we observe in the RPs for the solid [Figs. 2(g) and 2(h)], where we see that there are very small islands of dark blue points that are separated by red (or nearly red) points. As temperature increases, the increased velocities of atoms lead to faster decorrelation since the time of succes-

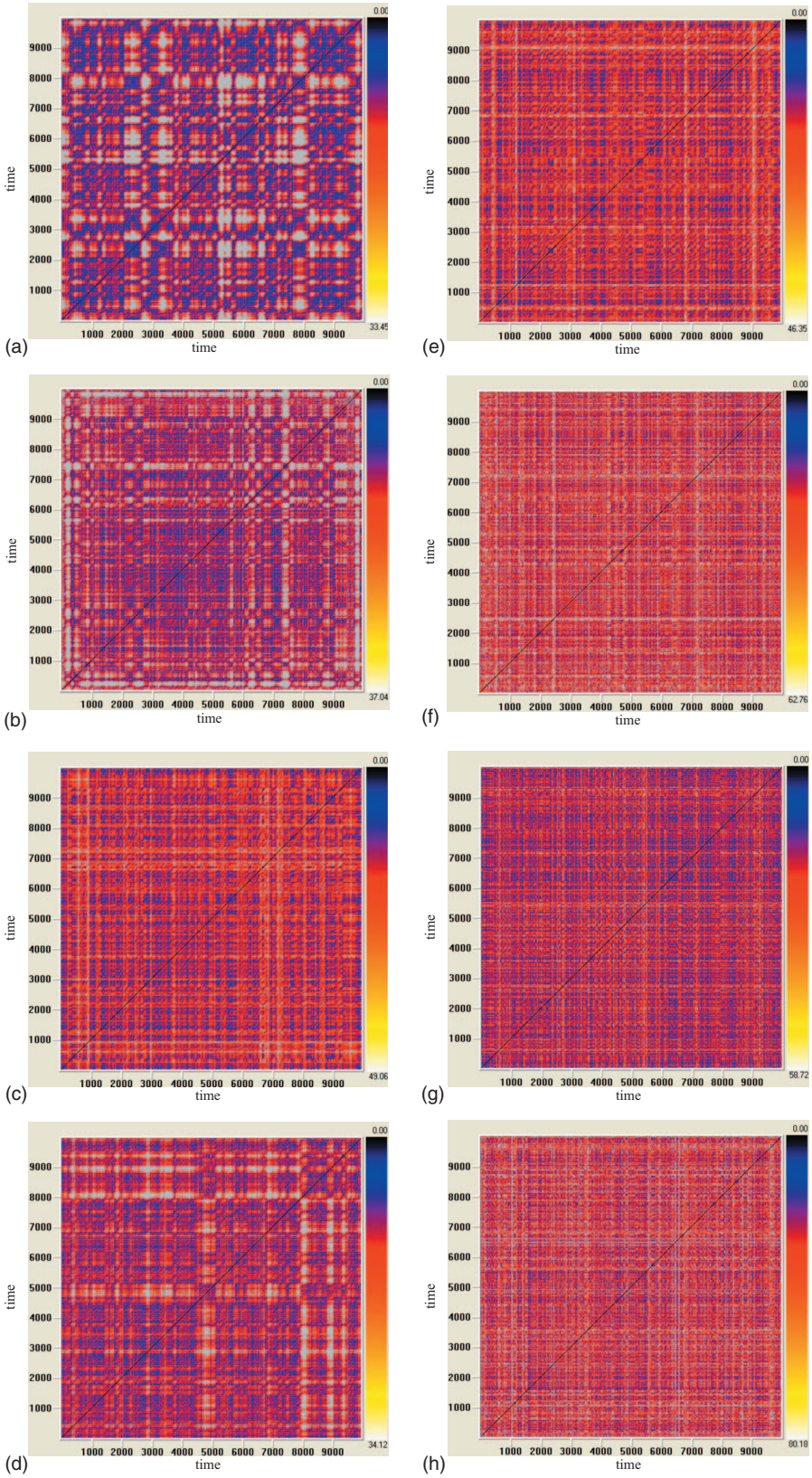


FIG. 2. (Color) Recurrence plots for various system densities and temperatures. (a) $T^*=1.5$ and $\rho^*=0.2$ ($\tau_d=17$); (b) $T^*=2.5$ and $\rho^*=0.2$ ($\tau_d=13$); (c) $T^*=1.5$ and $\rho^*=0.4$ ($\tau_d=16$); (d) $T^*=2.5$ and $\rho^*=0.4$ ($\tau_d=11$); (e) $T^*=1.5$ and $\rho^*=0.8$ ($\tau_d=11$); (f) $T^*=2.5$ and $\rho^*=0.8$ ($\tau_d=10$); (g) $T^*=1.5$ and $\rho^*=1.4$ ($\tau_d=4$); (h) $T^*=2.5$ and $\rho^*=1.4$ ($\tau_d=4$). (Time is in units of simulation time steps, i.e., $10^{-14}$ s.)

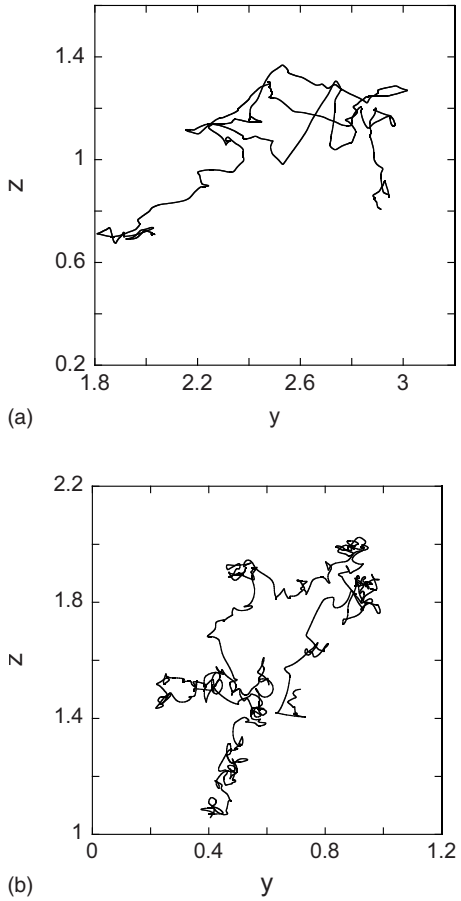


FIG. 3. Typical trajectories of atoms (projection on $y$-$z$ plane) in the liquid phase. (a) $T^*=1.5$ and $\rho^*=0.2$; (b) $T^*=1.5$ and $\rho^*=0.8$.

sive changes in the sign of the particle velocity gets smaller. As a result, the blue islands (indicating strongly correlated states) get smaller, while we have the appearance of gray regions corresponding to decorrelated microstates.

In the liquid, the situation is more complicated, since in this case atoms perform a more complex motion. Now atoms can be considered to reside in a kind of "cage" formed by their neighboring atoms. The boundaries of the cages are not rigid but, due to the motion of the atoms, they fluctuate. Due to the interactions, an atom moves within its cage (a kind of vibrational motion) and at some instances gets out of its cage and moves to another one. This motion is related to the diffusion process. Representative atomic trajectories of an atom at the lowest fluid density studied in the present work ($\rho^*=0.2$) are shown in Fig. 3(a) and at the highest density ($\rho^*=0.8$) in Fig. 3(b). In the high-density liquid, the atom spends some time around a given position before diffusing to a new position where again it spends some time, and so on. At low density, the atom is mainly diffusing. The change in system configuration due to a diffusing atom results in a new microstate that differs considerably from the previous one. Geometrically speaking, this means that in phase space the two points (states) will be relatively distant. On the other hand, when the atom remains within its cage the system configuration does not change significantly. However, the vibrational motion of the atom will result in collisions with the cage's boundaries. These collisions will have a characteristic time related to the time between successive changes of the velocity sign, which is in general an order of magnitude smaller than the characteristic times related to the diffusion events. In summary, both diffusional and vibrational components lead to the decorrelation of states, but at different time scales.

The macroscopic system density and temperature influence the degree of decorrelation between states by affecting how far and how fast an atom can travel without a change in the sign of its velocity. For fixed temperature we note that "blue islands" get larger as density is reduced [Figs. 2(e), 2(c), and 2(a)]. Of course, lower density means that diffusion dominates, i.e., hopping events are frequent and the time of flight increases along with the corresponding hopping distances. The denser the fluid the more restricted in the "cages" the atoms are, thus vibrations are predominant and loss of memory occurs faster, resulting in smaller "blue" islands immersed in red and gray points. An increase in system temperature leads to more energetic atoms which have higher probability to diffuse; they travel faster, collide faster, and thus result in smaller blue islands and fine-structured gray bands. Such behavior is in agreement with spectral and rescaled range analyses which both show a two-regime behavior (a vibration-dominated short time regime and a diffusion-dominated larger time regime) [8].

The points close to the diagonal (identity) line deserve special attention. The color of the pixels around the diagonal indicates the degree of recurrence in successive points (states). If there are recurrences we observe a kind of square structure with diagonal located on the main diagonal, which in our case will be blue-colored squares. We observe in Fig. 2(a) (lowest density and lowest temperature) that in fact there are such squarelike structures located along the diagonal. The size of these structures gets smaller as the density increases [Figs. 2(c) and 2(e)]. A similar behavior is observed also as temperature increases. We believe that this is related to the diffusional motion of the atoms since during diffusion the successive states are related and thus nearly recurrent. In the solid [Fig. 2(h)] there are very small such square blue structures due to the vibrational motion, where atoms change sign of the velocity very fast, and thus we have loss of correlation with the previous positions.

It is of interest to zoom on regions along the main diagonal. Figures 4(a)–4(d) contain representative magnified subregions along the diagonal of the lowest-density and -temperature fluid state. In this case there are structures of vertical and horizontal lines formed mainly by red points along with blue structures (of recurrent states) normal to the diagonal. The horizontal and vertical lines indicate that states do not change for some time, while the lines orthogonal to the identity line are indicative of an evolution of states similar at different times but with reverse time. The corresponding zooms for a representative solid state [Figs. 4(e)–4(f)] show a different structure consisting mainly of red and blue "lines" parallel to the diagonal and islands consisting of blue points. The lines parallel to the diagonal indicate that the evolution of states is similar at different time intervals. The time distance between these lines corresponds to some characteristic period. In our case, this distance is of the order of

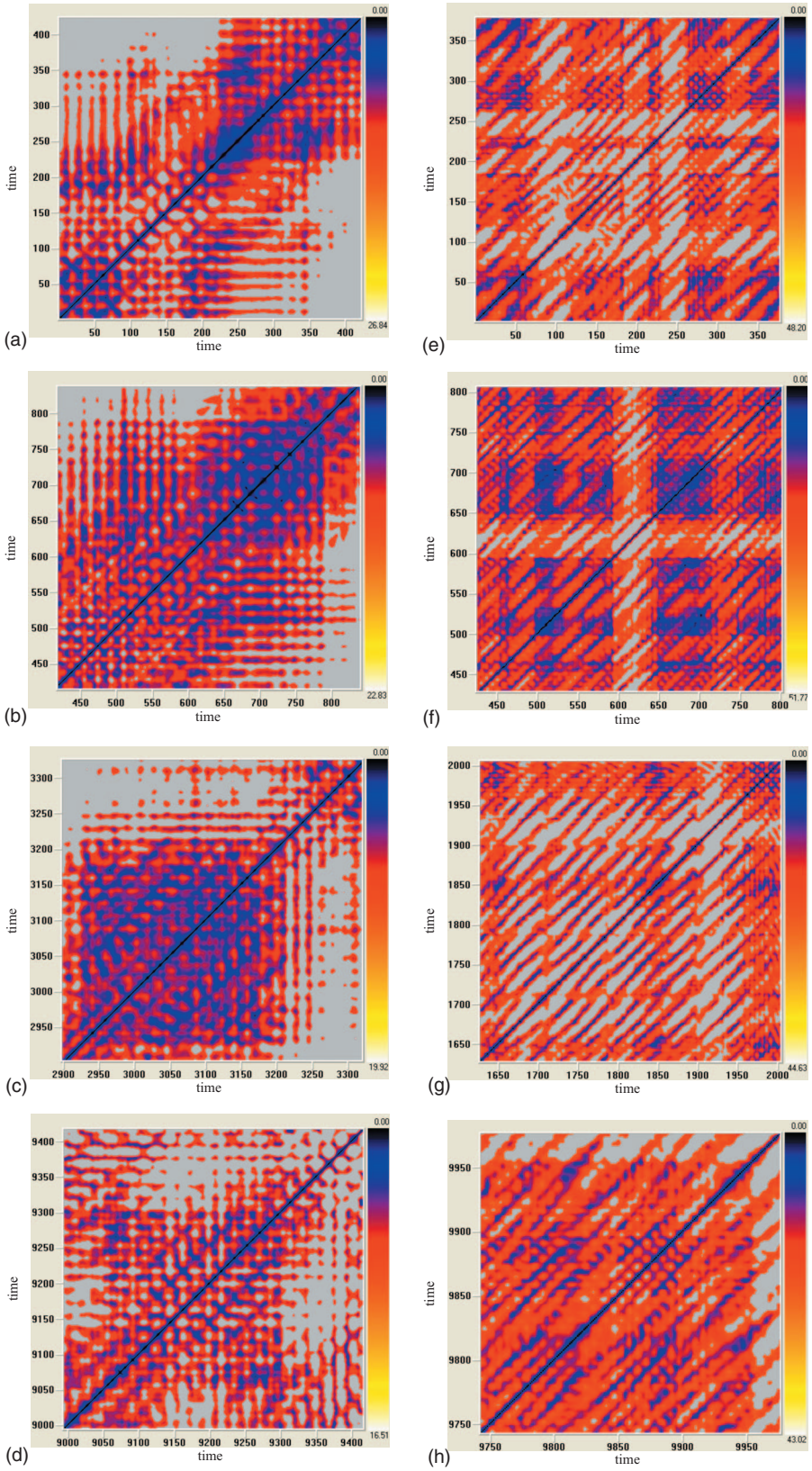


FIG. 4. (Color) (a)–(d) Zoom along the diagonal for the lowest fluid density [$\rho^*=0.2$, $T^*=1.5$, ($\tau_d=17$)]; (e)–(h) zoom along the diagonal for the solid state [$\rho^*=1.2$, $T^*=1.5$ ($\tau_d=6$)]. (Time is in units of simulation time steps, i.e., $10^{-14}$ s.)

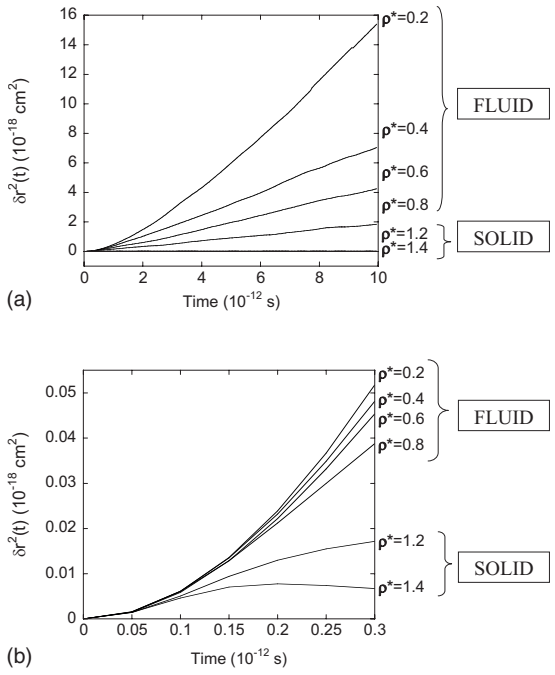


FIG. 5. (a) Mean square displacement at $T^*=1.5$ and various system densities. (b) Same as in (a) but zoomed at small time scale.

$20\delta t$, which corresponds to a frequency of a few terahertz, representative of the vibrational motion of the atoms in the solid. It is clear that the fine structure of RPs close to the main diagonal is quite different between the solid and liquid. In the liquid case the dominant characteristic is the existence of vertical and horizontal lines, while in the solid the dominant feature is the lines parallel to the main diagonal. This may be used as a signature of the phase characterization of the system (liquid or solid).

The average displacement of all atoms is quantified by the mean square displacement defined in Eq. (6). Figure 5 shows the computed MSD for several thermodynamic states. For fluid states, our results are in agreement, at least qualitatively, with the notion of Brownian motion. It is well known that in Brownian motion [31] there is a characteristic time $\tau=m/6\pi\eta\alpha$ that leads to two distinct limiting cases for the mean square displacement of the atoms.

(i) For times $t \ll \tau$, (inertia-dominated free flight regime)

$$\langle r^2 \rangle = |u_0^2| t^2 = \frac{kT}{m} t^2 \tag{10}$$

i.e., the mean square displacement is independent of the density and depends only on the temperature of the system.

(ii) For large $t$,

$$\langle r^2 \rangle = \frac{6kT\tau}{m} t = \frac{kT}{\pi\eta\alpha} t = 6Dt, \tag{11}$$

i.e., the MSD is proportional to temperature and inversely proportional to shear viscosity. In the equations above, $D$ is the self-diffusion coefficient, $m$ is the mass of the atom, $\alpha$ denotes the atom diameter, and $\eta$ is the fluid viscosity.

Computed MSDs for various system densities are shown in Fig. 5, where the distinct behavior predicted by the theory [Eqs. (10) and (11)] is reproduced.

Equation (11) allows us to relate computed MSD values with shear viscosity values for specific system densities and temperatures. We have analyzed the trends reported by Meier *et al.* [32] in their recent work on the shear viscosity of Lennard-Jones fluids and found good agreement with our MSD calculations.

When we zoom in on the MSD versus time plot [Fig. 5(b)] we observe that, up to time $t_1 \approx 0.6 \times 10^{-13}$ s, all the curves for various system densities collapse into one curve (at least at the scale of the figure). For the fluid states, the collapse to a single curve persists up to time $t_2 \approx 1.2 \times 10^{-13}$ s. If we zoom in on the recurrence plots of low- and high-density fluid (Fig. 6) we observe small islands of blue points ("highly" recurrent points) that are not evident at the resolution of Fig. 2. These small islands with characteristic length of the order of 5–10 pixels indicate that for very small times there are "recurrences" corresponding to times of the order of $(0.5–1.0) \times 10^{-13}$ s. It is remarkable that this characteristic time is comparable with the times up to which MSD curves in Fig. 5(b) collapse.

The characteristic structure of the RPs and its relation to the underlying physics of the system are confirmed by recurrence quantification analysis. Results concerning $\mathcal{R}_{\mathrm{DET}}$ are summarized in Fig. 7. For fluid states, $\mathcal{R}_{\mathrm{DET}}$ decreases at fixed temperature as the system density increases, and for fixed density as the system temperature increases. For each temperature, the calculated values of $\mathcal{R}_{\mathrm{DET}}$ for the four fluid states follow approximately a characteristic linearly decreasing trend. For the solid states, it appears that $\mathcal{R}_{\mathrm{DET}}$ approaches a temperature-dependent limiting value with a slight increase when the density of the solid is further increased.

We remind the reader that $\mathcal{R}_{\mathrm{DET}}$ measures the ratio of the number of recurrence points forming upward diagonal lines as a percentage of the total number of recurrence points in the RPs. The existence of diagonal lines indicates that the evolution of states is similar at different times and the process could be deterministic. We observe that, at a given temperature, $\mathcal{R}_{\mathrm{DET}}$ is higher in the fluid than in the solid, at least for the thermodynamic states studied here. This can be attributed to the fact that in the solid the only motion of the atom is the vibrational one, where during vibrations the microstates are related up to the time that an abrupt change in the direction of motion ("collision") occurs. In the fluid, we have a combination of diffusional and vibrational motion. This vibrational motion has characteristic times of the order of magnitude of the solid. However, as far as the diffusional component is concerned, the microstates of the system under study are more recurrent as long as an atom moves in a given direction (mean free path), and this leads to larger characteristic times, compared to those of the vibrational motion, and thus longer diagonal lines. At low densities atoms are freer to move and fewer collisions occur, thus successive microstates are more related (and thus are classified as recurrent). As a result $\mathcal{R}_{\mathrm{DET}}$ is high. Then, as density increases collisions among atoms become more frequent, thus resulting in fewer related microstates, fewer occasions of recurrent microstates,

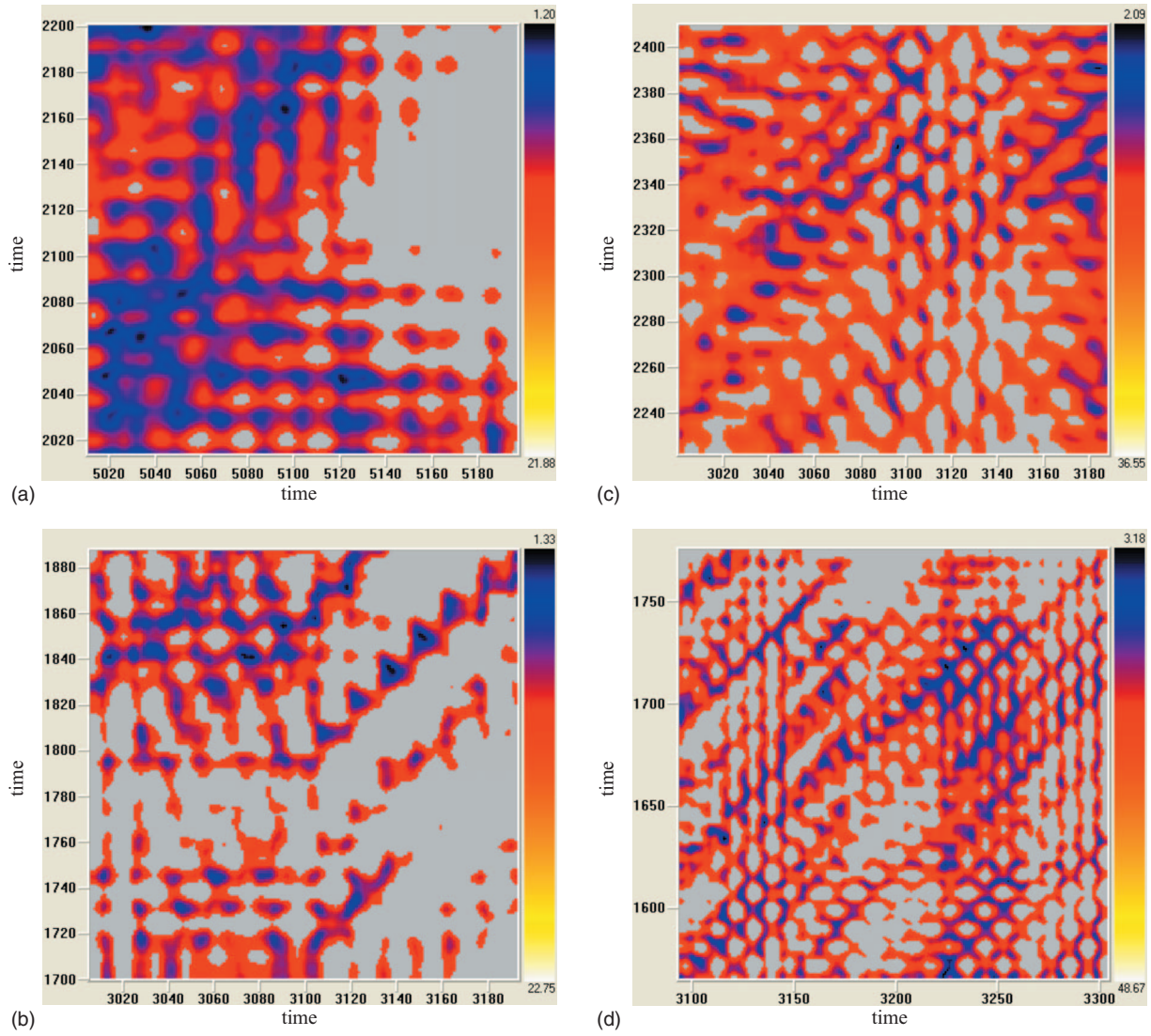


FIG. 6. (Color) Zoom at representative recurrence plots. (a) $T^*=1.5$ and $\rho^*=0.2$, (b) $T^*=2.5$ and $\rho^*=0.2$, (c) $T^*=1.5$ and $\rho^*=0.8$, and (d) $T^*=2.5$ and $\rho^*=0.8$. (Time is in units of simulation time steps, i.e., $10^{-14}$ s.)

and a reduction in $\mathcal{R}_{\mathrm{DET}}$. Now at a given density the increase of temperature results in faster motion of the atoms; thus collisions occur more often, the diagonal lines become shorter, and $\mathcal{R}_{\mathrm{DET}}$ is reduced.

Results concerning the maxline are summarized in Fig. 8. The observed behavior is consistent with the atomic motion discussed above. We can see from the results that, as temperature increases at a given density, the maxline is reduced, since as we have mentioned an increase in temperature results in atoms moving faster and thus colliding faster, and consequently the corresponding microstates become uncorrelated on shorter time scales. At given temperature, $\mathcal{R}_{\mathrm{DET}}$ reduces as density increases, since in a more dense environment collisions among atoms occur more often (thus faster) and the corresponding microstates become uncorrelated on shorter time scales again. We notice the dramatic drop in the value of the maxline between the states $\rho^*=0.8$ (fluid) and $\rho^*=1.2$ (solid). Maxline values are the most sensitive, among the indices examined, to the transition from liquid to solid. It is worth mentioning that the effect of temperature is important, since at the highest temperature studied the drop of the maxline is more important as a function of the system density.

As we have already discussed in Sec. II B, the maxline can be used as an estimator of $K_2$ entropy and thus of the lower limit of the positive Lyapunov exponents since $K_2 \leqslant \Sigma_{\lambda_i>0}\lambda_i$. Posch and Hoover [9] calculated the sum of the positive Lyapunov exponents for several fluid states from MD simulation output. Their calculations showed that this sum increases as the system temperature and density increases, indicating that the system becomes more chaotic. Thus our results are in qualitative agreement with those of Posch and Hoover.

The trapping time measures the average length of vertical lines of recurrence points and indicates for how long a system state does not change or changes slowly. In Fig. 9 we summarize the results for the TT for all thermodynamic states studied in the present work. It turns out that the TT

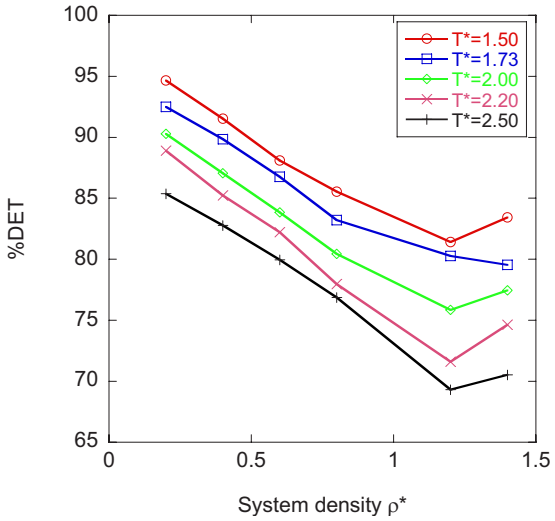


FIG. 7. (Color online) $\mathcal{R}_{\mathrm{DET}}$ obtained from the temperature time series at various system densities and temperatures (lines are only a guide to the eye).

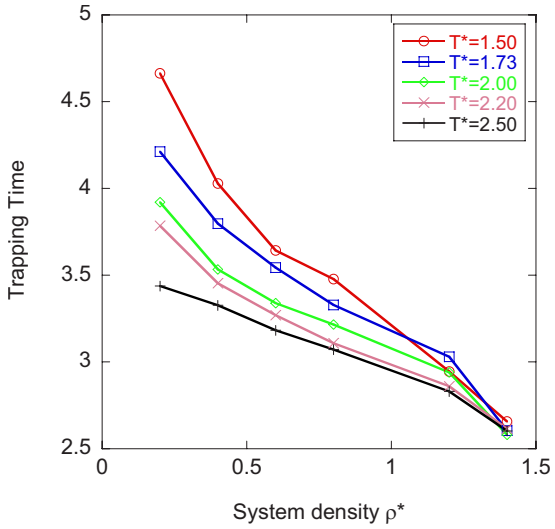


FIG. 9. (Color online) Trapping time obtained from the temperature time series at various system densities and temperatures (lines are only a guide to the eye).

decreases as temperature and density increase, similarly to the RQA descriptors ($\mathcal{R}_{\mathrm{DET}}$ and maxline) discussed above. At a given temperature, as the density increases and the atoms are more densely packed, the probability of the system remaining close to a given state is reduced due to the increased frequency of collisions. Similarly, at given density, as the temperature increases the probability of collisions increases and thus again the TT decreases. Although the variation of the TT with $\rho^*$ and $T^*$ shown in Fig. 9 is not very large, it is rather clear. With this latter in mind it is of interest to zoom in on the RPs (see Fig. 6) and focus our attention on the blue islands inside the red regions, which correspond to short-time correlations. These islands exist both at low and high values of system density and temperature, and their average vertical size seems to be of the order of five pixels, which is comparable with the TT values obtained. It seems also that their size follows a trend similar to that of the TT variation as a function of $\rho^*$ and $T^*$. These islands, whose size appears to be rather independent of the system thermodynamic state, seem to be an inherent characteristic of the system.

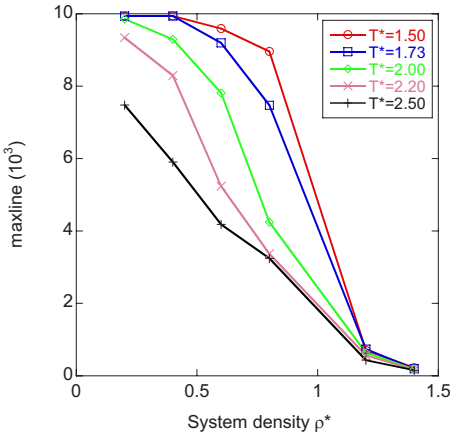


FIG. 8. (Color online) Maxline obtained from the temperature time series at various system densities and temperatures (lines are only a guide to the eye).

The transition from a homogeneous RP that corresponds to a solid phase to a more structured RP that corresponds to a liquid reflects in fact the transition from the vibrational motion of atoms (represented by the very small blue islands) to the combined vibrational and diffusional motion (represented by larger regions of recurrence points). The size of the RP structures seems to be larger at lower densities and lower temperatures. Thus one can envisage the use of RPs and RQA to identify the state of a system and locate a region where a phase transition occurs by the analysis of only one measured system property (observable), e.g., the instantaneous temperature.

## IV. CONCLUSIONS

In the present work, we have tried to establish the efficacy of recurrence plots and recurrence quantification analysis in gaining insight into molecular dynamics simulations, and to show the relation between the physics of the system under study and the visual as well as quantitative recurrence analysis results. Temperature time series of a Lennard-Jones system were recorded in various liquid and solid states, and the effect of system density and temperature on the corresponding RPs has been examined.

Low-density fluids generate RPs with a rather well-defined structure. This structure is gradually lost as the fluid density is increased and finally approaches the solid behavior, which gives rise to nearly homogeneous RPs. An increase in system temperature also leads to loss of the RP structure. These changes in RP characteristics are attributed to the distinct modes of motion of the atoms in the solid and fluid states. In the solid phase, the loss of structure is attributed to the vibrations of the atoms which lead to fast loss of memory at time scales comparable to the frequencies of vibration. In contrast, a fluid has a more complex atomic mo-

tion with both vibrational and diffusional components present. As atoms diffuse, they change microstates, and thus we have the appearance of significant white bands along with highly correlated motions. When the fluid temperature is raised, the increased probability of collisions leads to loss of correlation and gradual loss of structure in the RPs. Similarly, as the fluid density increases, atoms become more confined, diffusion events become less frequent and vibrational motions lead to faster loss of correlations, resulting in less structured RPs.

The quantitative descriptors of RQA shed more light on the observed behavior. $\mathcal{R}_{\mathrm{DET}}$, which measures the ratio of the number of recurrence points forming upward diagonal lines as a percentage of the total number of recurrence points in the RPs, decreases considerably as the system density and temperature increase. The maxline, which is proportional to the inverse of the largest Lyapunov exponent, follows the same tendency. In addition, the maxline marks very clearly the phase transition from liquid to solid behavior. Our computed maxline values in the liquid phase are in qualitative agreement with the results reported by Posch and Hoover [9] on the temperature dependence of the largest Lyapunov exponent of a Lennard-Jones fluid. Posch and Hoover found that the largest Lyapunov exponent increased as the system temperature increased, i.e., a consistent trend when compared with our maxline computtions. To the authors' knowledge no analogous study has been published for systems undergoing phase change. The trapping time also follows a trend consistent with the above behavior. The system under study gets trapped for very small times at a given state. At first glance the RPs miss this behavior, but, on closer examination, one detects a fine structure which manifests itself through well-defined small islands formed from points with high recurrence. It should be mentioned that the maxline is not the only quantitative descriptor that is able to distinguish between liquid and solid states. Indeed, values of all three RQA descriptors mark quite clearly the difference between liquid and solid states.

RPs and RQA constitute together a useful tool which can provide insight into the dynamics of atomic systems in a multitude of ways. Characteristic times related to the physical behavior of the system and in particular to the mean square displacement can be extracted from RPs. We can also extract qualitative information from RPs about the degree of atomic diffusion. The quantitative analysis of RQA can help us localize phase transitions in a more clear-cut way. This leads us to envision RP-based or RQA-based identification of a system phase in simulations or in experiments where we do not have access to full details about the system. However, it seems to us beneficial to quantify in new ways the wealth of information contained in RPs with a view to better capturing their signature quantities. To this end, work is under way to introduce RQA-based descriptors tailor-made for MD time series that will be based on either global or local measures.

## ACKNOWLEDGMENTS

This research has been partially supported by the program "PYTHAGORAS-EPEAEK II" Grant No. UTH-51908.04, jointly funded by the European Community and the Greek Ministry of Education.

[1] J. C. Sprott, *Chaos and Time-Series Analysis* (Oxford University Press, New York, 2003).
[2] H. Kantz and T. Schreiber, *Nonlinear Time Series Analysis*, 2nd ed. (Cambridge University Press, Cambridge, U.K., 2004).
[3] H. D. I. Abarbanel, *Analysis of Observed Chaotic Data* (Springer, Berlin, 1996).
[4] J.-P. Eckmann, S. O. Kamphorst, and D. Ruelle, Europhys. Lett. **4**, 973 (1987).
[5] C. L. Webber, Jr. and J. P. Zbilut, J. Appl. Physiol. **76**, 965 (1994).
[6] D. C. Rapaport, *The Art of Molecular Dynamics Simulation* (Cambridge University Press, Cambridge, U.K., 1995).
[7] M. P. Allen and T. J. Tildesley, *Computer Simulation of Liquids* (Clarendon Press, Oxford, 1987).
[8] T. E. Karakasidis and A. B. Liakopoulos, Physica A **333**, 225 (2004).
[9] H. A. Posch and W. G. Hoover, Phys. Rev. A **38**, 473 (1988).
[10] H. A. Posch and W. G. Hoover, Phys. Rev. A **39**, 2175 (1989).
[11] A. Giuliani and C. Manetti, Phys. Rev. E **53**, 6336 (1996).
[12] C. Manetti, M.-A. Ceruso, A. Giuliani, C. L. Webber, Jr., and J. P. Zbilut, Phys. Rev. E **59**, 992 (1999).
[13] J. L. Lebowitz, J. K. Percus, and L. Verlet, Phys. Rev. **153**, 250 (1967).
[14] B. L. Holian and D. J. Evans, J. Chem. Phys. **78**, 5147 (1983).
[15] L. Verlet, Phys. Rev. **159**, 98 (1967).
[16] N. Marwan, M. C. Romano, M. Thiel, and J. Kurths, Phys. Rep. **438**, 237 (2007).
[17] C. L. Webber, Jr. and J. P. Zbilut, in *Tutorials in Contemporary Nonlinear Methods for the Behavioral Sciences*, edited by M. A. Riley and G. Van Orden (2005), Chap. 2, pp. 26–94, http://www.nsf.gov/sbe/bcs/pac/nmbs/nmbs.pdf
[18] J. S. Iwanski and E. Bradley, Chaos **8**, 861 (1998).
[19] N. Marwan, Ph.D. thesis, University of Potsdam, 2003 (unpublished).
[20] N. Marwan, N. Wessel, U. Meyerfeldt, A. Schirdewan, and J. Kurths, Phys. Rev. E **66**, 026702 (2002).
[21] J. P. Zbilut, A. Colosimo, F. Conti, M. Colafranceschi, C. Manetti, M. C. Valerio, C. L. Webber, Jr., and A. Giuliani, J. Proteome Research **3**, 1243 (2004).
[22] A. Giuliani, R. Benigni, J. P. Zbilut, C. L. Webber, Jr., P. Sirabella, and A. Colosimo, Chem. Rev. (Washington, D.C.) **102**, 1471 (2002).
[23] E. Cazares-Ibanez, G. A. Vazquez-Coutino, and E. Garcia-Ochoa, J. Electroanal. Chem. **583**, 17 (2005).
[24] F. Strozzi, J.-M. Zaldiovar, and J. P. Zbilut, Physica A **312**, 520 (2002).
[25] A. Fabretti and M. Ausloos, Int. J. Mod. Phys. C **16**, 671 (2005).

[26] N. Marwan and A. Meinke, Int. J. Bifurcation Chaos Appl. Sci. Eng. **14**, 761 (2004).
[27] M. A. Riley, R. Balasubramaniam, and M. T. Turvey, Gait and Posture **9**, 65 (1999).
[28] E. I. Vlahogianni, M. G. Karlaftis, and J. C. Golias, Transp. Res., Part C: Emerg. Technol. **14**, 351 (2006).
[29] L. L. Trulla, A. Giuliani, J. Zbilut, and C. L. Webber, Jr., Phys. Lett. A **223**, 255 (1996).
[30] E. Kononov, computer code VRA, http://home.netcom.com/~eugenek
[31] D. A. McQuarrie, *Statistical Mechanics* (Harper Collins, New York, 1976).
[32] K. Meier, A. Laesecke, and S. Kabelac, J. Chem. Phys. **121**, 3671 (2004).